UNIVERSITY OF HELSINKI REPORT SERIES IN PHYSICS

HU-P-D108

Stopping Power for Ions and Clusters in Crystalline Solids

Jarkko Peltola

Accelerator Laboratory
Department of Physics
Faculty of Science
University of Helsinki
Helsinki, Finland

ACADEMIC DISSERTATION

To be presented, with the permission of the Faculty of Science of the University of Helsinki, for public criticism in main Auditorium of the Department of Physics, on Dec 20th, 2003, at 10 o'clock noon.

HELSINKI 2003

ISBN 952-10-0939-X (printed version)
ISSN 0356-0961
Helsinki 2003
Yliopistopaino

ISBN 952-10-0940-3 (PDF version)
http://ethesis.helsinki.fi/
Helsinki 2003
Helsingin yliopiston verkkojulkaisut

J. Peltola: **Stopping power for ions and clusters in crystalline solids** University of Helsinki, 2003, 38 p.+appendices, University of Helsinki Report Series in Physics, HU-P-D108, ISSN 0356-0961, ISBN 952-10-0939-X (printed version), ISBN 952-10-0940-3 (PDF-version)

Classification (INSPEC): A3410
Keywords (INSPEC): Molecular dynamics method, ion implantation, electronic stopping

ABSTRACT

The modern microelectronics industry has been rapidly growing over the last two decades. The constant need for better components demands accurate knowledge of the physical processes on the atomic level. One of the most important quantities in the field of materials physics is the stopping power of ions inside materials. In this research field, computer simulations are used extensively.

In this thesis, new models for calculating electronic stopping of ions in the framework of molecular dynamics computer simulations have been developed. The calculation method uses the local electronic enviroment inside crystalline silicon and nonlinear results from the density functional theory. A comparison to experimental data is done by comparing the experimental and simulated range profiles of ions. An extension to the low energy stopping in a multicomponent target (GaAs) is studied as well. The stopping calculation is extended to higher energies for light ions.

Effects of the silicon structure on the range profiles have been studied for the damage accumulation process due to high implantation fluences. Finally, the stopping of small Au clusters in copper and silicon have been studied.

The main findings are that we found the reason for the experimentally observed broadening of the range profile of Au clusters in Cu, and that we can now predict the range profiles of low-energy ions in silicon for a wide range of different implantations more accurately than what had been possible earlier.

CONTENTS

1 INTRODUCTION

Exponential growth in the microelectronic components industry has created a constant need for new and better materials tailored for specific purposes. Materials properties can be optimized to match technical requirements better. The mechanical [1] and electrical (leading to optical [2]) properties of a material change when impurity atoms are present in the structure. Ion beams can be used as a tool for adding the impurities. The chosen impurity atoms are accelerated to a desired energy and implanted into the material. Due to the statistical nature of ion penetration, the ions form a distribution inside the material, which is called the concentration profile or the range profile. In the semiconductor industry, it is important to know the exact ion distribution to achieve the properties desired.

In order to find out what is happening on atomic length scales, we need good theoretical knowledge about the fundamental interaction processes and aid from computer simulations, which are widely used in studying materials and developing new components. The simulations can give a detailed view of the atom movement and thus give an insight into the atomic processes and perhaps even interpret experimentally observed phenomena.

The question of atom movement inside materials has traditionally been reformulated into a question of how much energy the projectile loses in a certain distance traveled. This quantity is called the stopping power. When the stopping power is known for an ion as a function of ion velocity, the penetration depth scales of the ion can be linked to its energy loss. The stopping is used to predict the range profiles of the implanted ions inside materials and to determine the absolute depth scales in the analysis of the target structures by the Rutherford Backscattering Spectrometry (RBS) and Elastic Recoil Detection Analysis (ERDA) techniques [3]. The stopping of the ion is not a fundamental quantity in the sense that it is not a unique function of energy. It is a result of many different velocity dependent statistical events that lead to an average loss of the kinetic energy of the ion. There is a considerable standard deviation around this average. The theory of the slowing down of an ion dates back to Bohr’s pioneering paper in 1913 [4]. Since then, a constant development of stopping theories has been going on for a nearly hundred years, with help from developments in microelectronics and atomic scale analysis techniques.

The stopping of an ion is theoretically best known when the charge state of the ion does not change and the target material is amorphous [5]. In this case, the range profile of the ions can be predicted accurately by analytical methods or by the use of transport theory and Monte Carlo (MC) simulations. This is due to the fact that the important quantities affecting the stopping, the electron and atom densities, can be treated as constants [6]. But when the target has a crystalline structure, like silicon, or the ion charge is not constant or the ions belong to a cluster, the stopping power is poorly known

and further theoretical research is required. Because of the inhomogeneous structure of the crystal, the range profiles are not symmetric distributions as assumed in the early analytical models. Effects such as channeling make the range profiles far from Gaussian-shaped. The linearity assumptions for the electron gas responses used in the early stopping models must also be abandoned. Thus, we need accurate simulations methods and better models for the stopping to predict the range profiles of ions in crystalline materials.

2 PURPOSE AND STRUCTURE OF THIS STUDY

The purpose of this study is to improve the calculation of stopping powers of crystalline solids. Nowadays Molecular Dynamics (MD) methods are used to predict the range profiles of the ions. The main technological interest for accurate prediction of range profiles lies in the semiconductor materials used in integrated circuits. This is the reason to primarily study silicon in this thesis.

This thesis consists of a summary and six articles that were published or accepted for publication in refereed international scientific journals. The articles are referred to by Roman numbers.

Short summaries of the original papers

Paper I: Electronic stopping calculated using explicit phase shift factors, J. Sillanpää, J. Peltola, K. Nordlund, J. Keinonen and M. J. Puska, *Phys. Rev. B* **63**, 134113 (2001).

> In this paper, we use direct Density-Functional-Theory (DFT) results and the nonlinear theory to calculate electronic stopping power of c-Si for different low-energy heavy ions. The simulated range profiles are in good agreement with the experimental results in all implantation directions, except the <110> channel.

Paper II: Effects of damage build-up in range profiles in crystalline Si; molecular dynamics simulations, J. Peltola, K. Nordlund and J. Keinonen, *Nucl. Instr. Meth. Phys. Res. B* **195**, 269 (2002).

> We use full MD simulation results for the amorphization of the c-Si structure to describe the damage accumulation in the ion range simulation. The implantation fluence and the deposited nuclear energy are self-consistently determined in the simulation. No free parameters are used.

Paper III: Heat spike effect on the straggling of cluster implants, J. Peltola and K. Nordlund, *Phys. Rev. B* **68**, 35419 (2003).

Experimental results by H. H. Andersen [7] on the implantation of small low-energy gold clusters in Cu and amorphous Si (a-Si) show that the range profile broadens in Cu, but not in a-Si, as the cluster size increases. We study the increase of straggling in the range profiles with MD simulations. The simulations show that the heat-spike created by the clusters in Cu, but not in Si, is the reason for the increase in the straggling values.

Paper IV: Explicit phase shift factor stopping model for multi-component targets, J. Peltola, K. Nordlund and J. Keinonen, *Nucl. Instr. Meth. Phys. Res. B* **212**, 118 (2003).

The previously developed model for electronic stopping power of slow ions is extended to multi-component targets. GaAs was the target and spherically symmetric electron distributions of atoms were used to calculate the free-electron-gas electronic stopping. The maximum and the most probable ranges in the simulated concentration profiles are in good agreement with experiments for all ions in all implantation directions.

Paper V: Electronic stopping power calculation method for molecular dynamics simulations using combined Firsov and free-electron-gas models, J. Peltola, K. Nordlund and J. Keinonen, *Radiation Effects and Defects in Solids* submitted for publication (2003).

The electronic stopping of a slow ion is divided into two local contributions. The electron exchange between the ion and target atoms during close collisions is calculated using the Firsov model. The momentum exchange between the ion and valence electrons is calculated using the free-electron-gas model, where the electron density is taken from a three dimensional valence electron distribution of a silicon crystal. The problem of too low an electron density experienced locally by a point-like ion in the middle of the <110> crystal channel is corrected with an effective density. The simulations give good results compared to the previous version of our model and the experiments.

Paper VI: Molecular dynamics study on stopping powers of channeled He and Li ions in Si, J. Peltola, K. Nordlund and J. Keinonen, *Nucl. Instr. Meth. Phys. Res. B* accepted for publication (2003)

This study gives results from the extension of the local free-electron-gas stopping model for high velocities. The stopping of light ions like He and Li are calculated in silicon channels using the MD method. The phase-shifts are determined using a recent extension of the Friedel Sum Rule. Results give a decent agreement with the experimental stopping measurements, but the underestimation of the stopping in the <110> channel is again seen.

All the papers published for this thesis are results of group work done in the Accelerator Laboratory. The author of this thesis has done the major part of the simulations and writing in the papers. In paper I, the basis of the calculation method of the electronic stopping power for low-energy ions in MD

simulations is developed. In paper II, the effect of damage accumulation in the originally crystalline Si (c-Si) on the depth distribution profiles is modeled with a new method. Paper III presents a solution for the broadening of the depth profile for gold clusters implanted in copper and the cluster stopping is discussed. In paper IV, the electronic stopping model is extended to multi-component targets and in paper VI to higher energies for light ions. A use of one adjustable parameter and the distinguishing of the electronic stopping to elastic and inelastic contributions are presented in paper V.

3 STOPPING POWER

3.1 Slowing down of ions in materials

An energetic ion[1] penetrating in a medium interacts with the target atoms. It collides with the nuclei and electrons of the target. The interactions lead to a loss of the ion's energy. In the energy range of 0 - 10 keV/amu, in which we are mainly interested, the energy loss per unit length i.e. the **stopping power**, can be divided into nuclear stopping and electronic stopping terms [5]. The nuclear stopping governs the energy losses caused by elastic collisions between the ion and the nuclei of atoms in the target. The electronic stopping term governs the energy losses caused by the electronic interactions, which can be further divided into several different contributions depending on the nature of the interaction. Hence, the stopping power (or slowing down force) can be written as

$$S = \left(\frac{dE}{dx}\right) = \left(\frac{dE}{dx}\right)_{nuclear} + \left(\frac{dE}{dx}\right)_{electronic}. \tag{1}$$

For high energies (>10 MeV/amu), contributions coming from nuclear reactions and relativistic corrections have to be taken into account. However, they can be neglected in the context of this thesis as the particle velocities are far below the velocity of light.

These stopping contributions cause the energetic ion to stop at some predictable distance inside the medium. Formally this can be written as [8]

$$R = \int_U^E \frac{dE'}{S(E')}, \tag{2}$$

where E is the initial energy, U the visibility threshold for the track and R is the *range* of the ion. If $S(E')$ is the mean stopping power value, we obtain the mean range for the ions. However, due to

[1] To distinguish between the target and projectile atoms, the incoming projectile is referred to as an ion in this study.

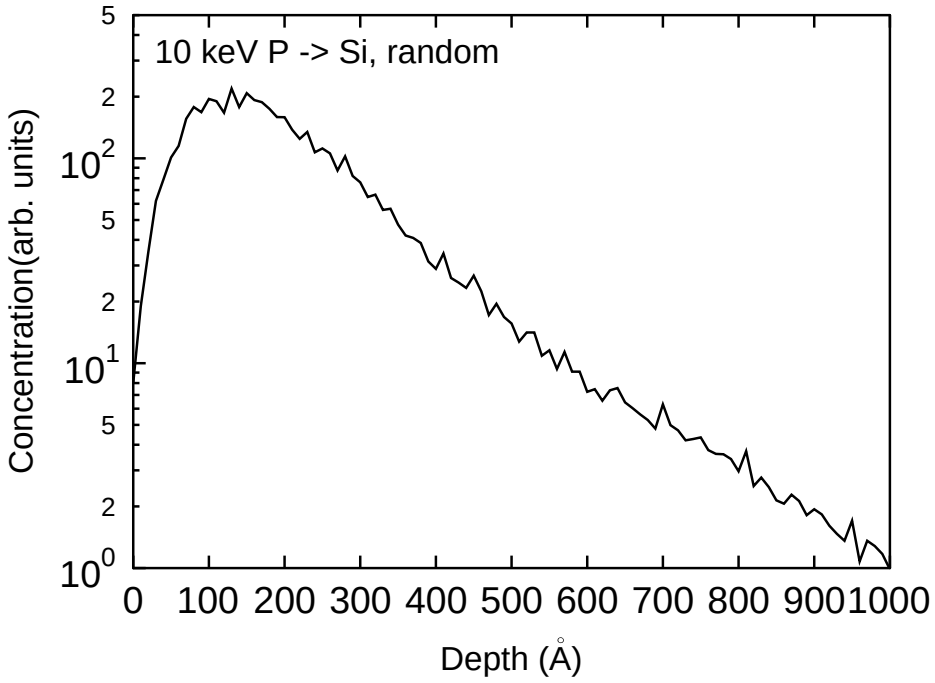

Figure 1: Example of a simulated range profile for 10 keV P ions implanted in Si in a non-channeling ("random") direction. A logarithmic y-scale is used to emphasize the extension of the range profile deep in the material ("tail"). The implantation of 5000 real ions and 15247 virtual ions (sect. 4.3, REED) is simulated to obtain the desired accuracy for the distribution.

the statistical nature of the stopping of an ion, we do not obtain only one value for the range but a distribution of ranges. The range profile is often described by a mean projected range $\overline{R}$ and straggling σ of the distribution.

The range profile is an important result, because it describes the concentration distribution of implanted doping atoms. The concentration level affects, for example, the electrical properties of semiconductor materials [1, 9]. A typical range distribution is illustrated in Fig 1.

Numerical calculations of the range as a function of ion energy have originally been performed by Lindhard, Scharff and Schiøtt (LSS-theory) [10]. Their theory can predict ranges and stragglings of ions in non-crystalline materials, which as a first approximation leads to Gaussian range profiles [11]. Because of the anisotropy of crystalline materials used in the semiconductor industry, computer simulations are needed to determine accurate range profiles.

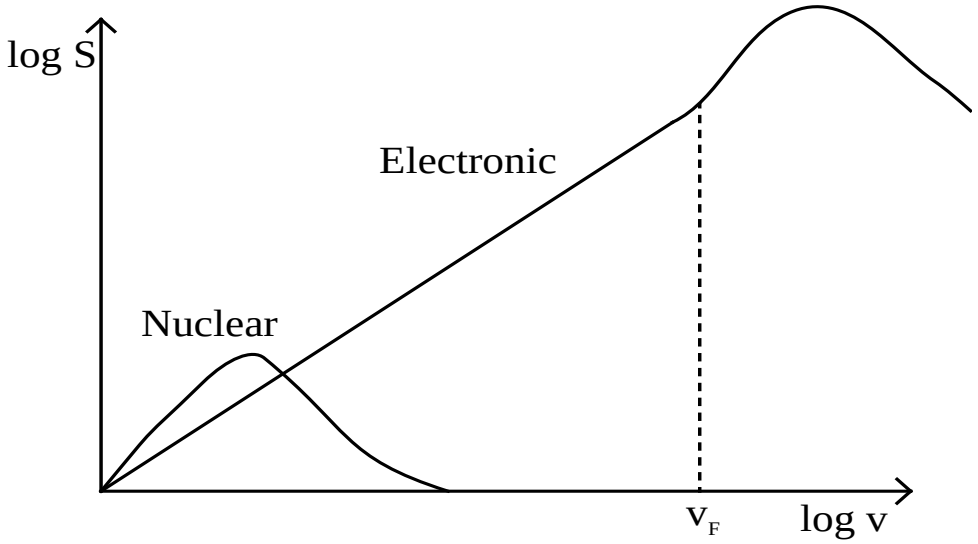

Figure 2: Schematic behavior of the nuclear and electronic stopping as a function of ion velocity.

3.2 Nuclear stopping

The nuclear stopping is a sum of the energy losses of a moving ion due to its elastic collisions with the target nuclei. The energy that an ion loses is converted to heat in the slowing down material as the atoms spread the kinetic energy in series of collisions, namely in collision cascades. A common feature for all ions is that the nuclear stopping as a function of ion energy has a maximum at a relatively low energy (of the order of 1 keV/amu) and that the nuclear stopping of the ion decreases as the energy of the ion increases. This means that the nuclear stopping is important only for low ion velocities. Analytically, the nuclear stopping of an ion can be integrated if one knows the statistics of energy transfer in atomic collisions. In modern computer simulations, the nuclear energy loss comes automatically into the picture due to the force interaction between the ion and the atoms, and an explicit analytical form is not needed at all.

3.3 Electronic stopping

Electronic stopping is a common term for the energy loss caused by all electronic processes. It originates from several different contributions depending on the type of the interaction. Ions moving faster than $\sim$ 1 keV/amu lose kinetic energy mainly via electronic stopping (see Fig. 2) [12].

When an ion moves inside the material, it collides with the electrons of the material, which can be either bound or free. In metals the electrons are divided into bound core electrons and free conductive electrons. In semiconductors, the valence electrons are not free, but are so loosely bound that they can be considered to be free in the electronic stopping framework used in this thesis.

If the ion is moving slowly, it carries all of its electrons with it. If the ion is moving faster than the fastest target electrons, it loses all its electrons and is completely ionized. These cases are the theoretically best understood ones. An ion moving slowly loses energy only to the free electrons of the target due to momentum exchange with them. Due to the forbidden energy levels, this results in a linear dependence of the stopping on velocity [13]. A high velocity ion can be considered to be a point-like charge, which can collide with all the electrons in the target. The stopping is then inversely proportional to the square of the ion velocity [14].

When the ion velocity is between these two cases, the ion is partially stripped leading to a considerably more complicated description [15], because the ion may lose electrons to, and capture them from, the medium.

The possible phenomena contributing to the electronic stopping in the velocity region well below the light velocity are:

(S1) momentum exchange in a collision between the ion and a free electron in the target material,

(S2) ionization of the ion,

(S3) the ion captures an electron,

(S4) (de-)excitation of the ion,

(S5) (de-)excitation of a target atom,

(S6) ionization of a target atom,

(S7) collective effects such as the polarization or the plasmon excitation

The electronic stopping is also divided into two different terms: electronic stopping during the collisions of the ion and atom and electronic stopping between the ion-atom collisions. The latter electronic stopping refers to the constant slowing force acting on the ion due to the momentum exchange with the electrons in the material (S1 in the list above). The former refers to the electron exchange between the atom and the ion in close collisions (for non-ionizing energies: S4 and S5). The importance of the different contributions to the total electronic stopping power depends on the ion velocity.

For high ion velocities all the electrons in the target take part in the slowing down process and the ionization processes must be taken into account. Processes like the ion-electron recombination greatly depend on the associated possibility of absorbing the neutralization energy [16]. Thus the velocity region of the ion (velocity v and atomic number Z_1) is divided into three main regions:

1. **Low-velocity region**, where the ion velocity v is below the Bohr velocity v_0 (in the electron gas theory the limit is commonly the Fermi velocity v_F) of the target electrons i.e. the velocity of the fastest electrons in the material. The ion is called *slow*.
2. **High velocity region**, where $v > v_0 Z_1^{2/3}$. The ion is called *fast* or *swift*.
3. **Intermediate velocity region**, which is the intermediate area between the low and high velocities, $v_0 < v < v_0 Z_1^{2/3}$,

where $v_0 Z_1^{2/3}$ is the mean velocity of the electrons filling the levels of a neutral atom with nuclear charge Z_1 obtained from the Thomas-Fermi statistical theory [6].

In this thesis, we are mostly interested in the low-velocity region (papers I,II,IV,V), which usually means ions moving with velocity *much* below the Fermi velocity of the electrons of the target material. In this case, the ion can not be ionized. The electronic stopping power is then calculated taking into account only the effects S1, S4 and S5, from which S1 is the most important [17]. Theoretical knowledge in this region has improved in the last two decades due to the development of nonlinear electron gas models. The main reason for the interest of this region is the extensive use of low energy ion implantation in the semiconductor industry.

In the intermediate region, ions lose or capture electrons. This velocity region is the most difficult to describe theoretically, because all the different corrections listed above (S1-S7) must be evaluated for the ion. The heavier the ion, the more electrons participate in the exchange processes. This leads to a stopping categorization, not only in terms of the ion velocity, but of the atomic numbers of the ion Z_1 and the target atoms Z_2 [18]. The quantized electron structures are different for different atom types and this affects the electronic energy loss phenomena. The different electronic stopping regions for light and heavy targets are shown in Fig. 3 as a function of Z_1. An interesting feature of the interaction of the electron shells appears as the stopping of an ion (Z_1) fluctuates along Z_2 and vice versa [19–21]. These phenomena are called the Z_1/Z_2-oscillations. The electronic structure brings Z dependent effects to the low-velocity region as well[22].

The electron capture and loss processes (S2 and S3) can have a notable contribution on the total stopping in the intermediate region. For example, it is calculated to cause 15 % of the electronic stopping power for helium ions at metallic electron densities in the intermediate velocity region [24].

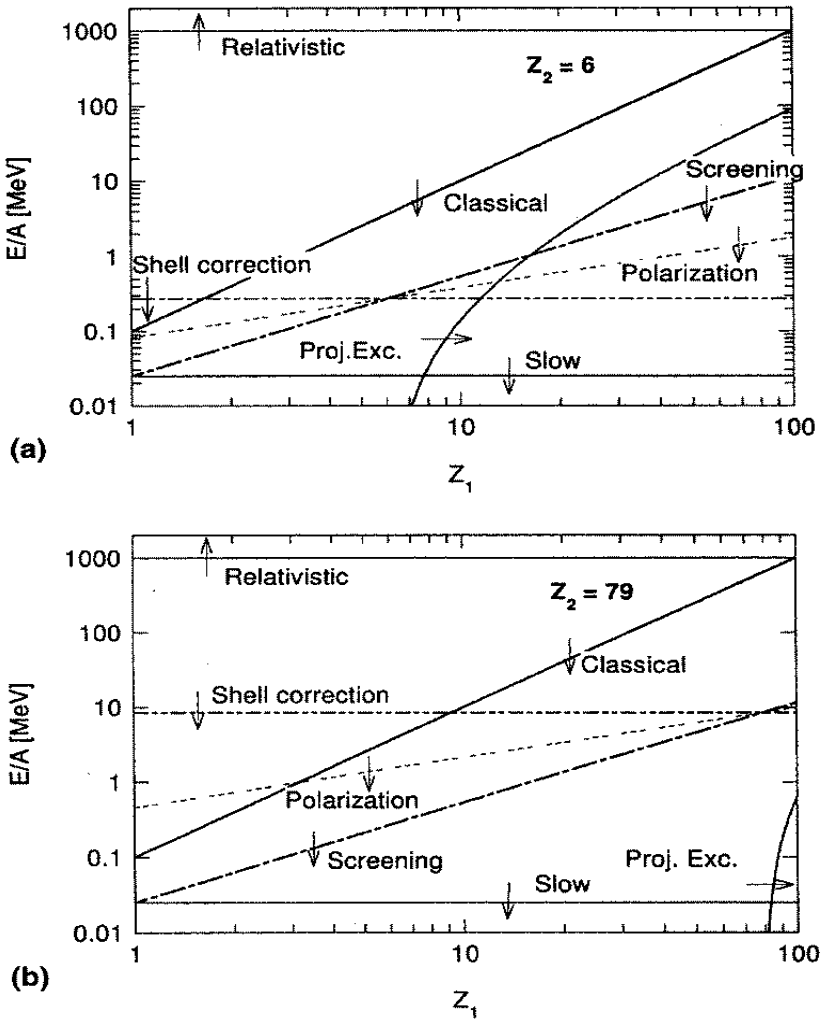

Figure 3: Approximate limits for different stopping regimes in carbon (a) and gold (b) targets [23]. The lines indicate rough upper limits, except for the relativistic, a lower limit, of different regions. The horizontal lines for 'relativistic' and 'slow' areas indicate the highly relativistic and the slow ($v < v_0$) ion limits. The 'classical' means the transition from the Bethe (quantal perturbation model) to Bohr (classical orbit model) regime and the 'screening' marks the pronounced static projectile screening (the potential of the ion is screened by its electrons). Polarization (S7), projectile excitation (S4) and the shell correction limits are also marked.

If the ion is swift and has lost all of its electrons, the question of stopping becomes the knowledge of the interaction between the bare nucleus and all the electrons in the target. Taking into account the intrinsic motion of the target electrons is called the shell-correction and its importance grows with increasing v and Z_2 [25, 26]. The stopping of a swift ion is purely electronic and it is theoretically relatively accurately known [27]. This region has been much studied over the years because of the needs of ion beam analysis. It has lead to sufficiently accurate stopping tables for a variety of ions in different materials. From the theoretical point of view, some crucial approximations are justified only

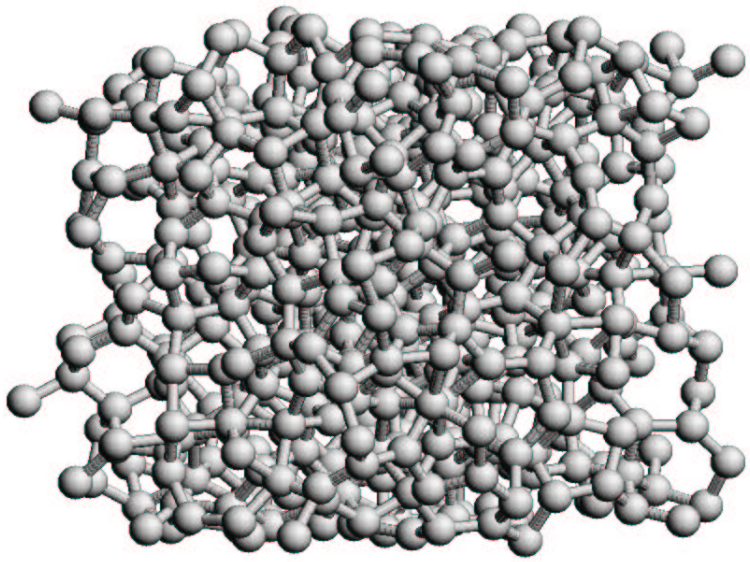

Figure 4: A piece of an amorphized [29]silicon crystal seen near the original <110> direction.

in this velocity region [28], which ease the calculations.

Because of the complex interactions taking place during a collision of two atoms, electronic stopping is still not completely understood, especially in the intermediate region.

3.4 Effect of the target structure

The crystalline structure of the target material has a large effect on the stopping and therefore on the range profiles [30, 31]. If the structure is amorphous (Fig. 4), the atoms are homogeneously and isotropically distributed. The stopping has no dependency on the direction of the ion movement. This means that the range profile has a symmetric, Gaussian form, which has a peak at the mean range [30]. The analytical calculations for the stopping of the ions and predicting range profiles are easiest to do for this type of materials.

In a crystalline structure, atoms form a periodic lattice, which forms rows of atoms and empty spaces depending on the viewing direction (Fig. 5). The same structure can appear to be a closed or open. The ion movement is very much direction dependent, because the densities of the atoms and electrons depend on the direction. The effect of this on the range profiles is illustrated in Fig 6.

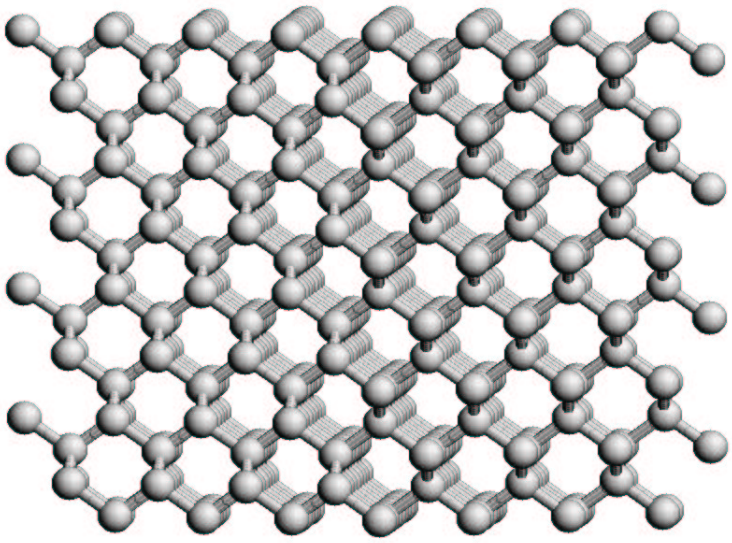

Figure 5: A piece of an ideal silicon crystal seen near the <110> direction.

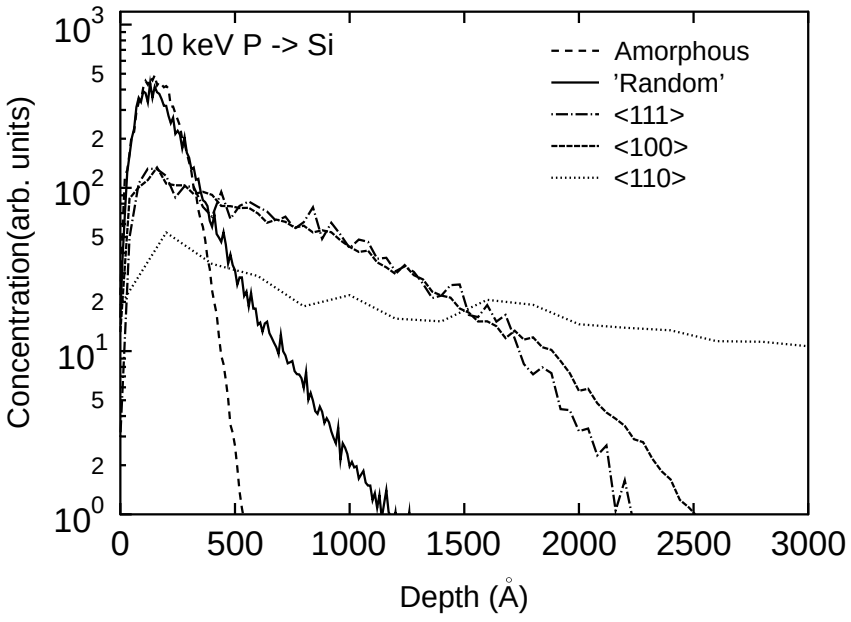

Figure 6: Comparison of the simulated range profiles of 10 keV P ions implanted in different crystal directions of Si.

In a channel formed by rows of atoms, the ion can move long distances without close collisions between the target atoms (Fig. 7). This is not simply a transparency phenomena as the trajectories of these ions are actually steered by a series of glancing collisions with the atom rows. This means

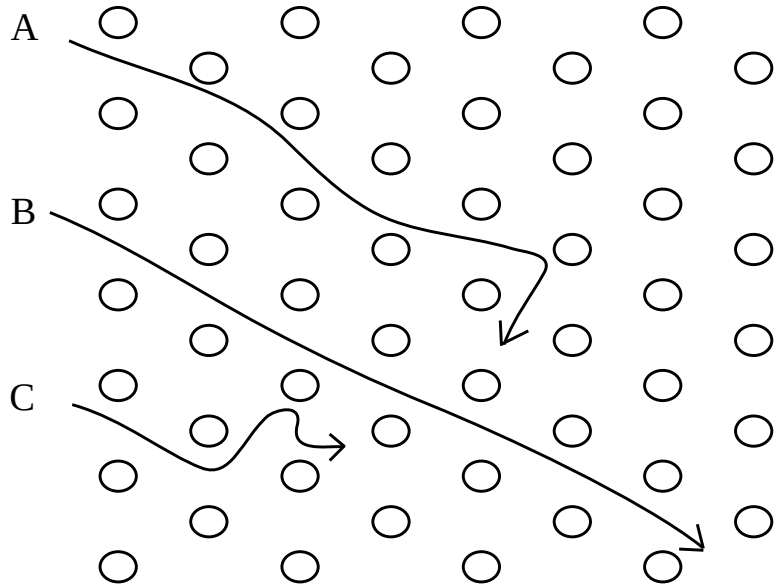

Figure 7: Examples of different behavior of ions implanted in crystalline materials. Ion (A) is moving in a channel for a short distance and is then dechanneled due to a close collision. Ion B is properly channeled and is moving a much longer distance than the ion C, which is randomly colliding with the target atoms.

that the nuclear stopping is much lower in these channels compared to the other directions. This phenomena is called *channeling*. The electron density in a channel is usually lower than the average density and leads to a lower electronic stopping than in a non-channeling direction. Theoretically, it can be explained that the ions are channeled if their impact vector is within some critical angle to the channel direction [32].

Due to the channeling and various types of anomalous diffusion of the ions, the range profiles are often not Gaussian [30].

4 CALCULATIONS OF ION SLOWING DOWN

4.1 Analytical models

Analytical models start from a picture in which an ion collides with atoms in a structureless material, without any correlation effects. The focus is not the ion trajectory, but the statistics of the energy transfer. This is defined by the cross section σ. If a particle with energy E moves a small distance ΔR in a random media of atomic density N, the probability dP of undergoing a collision with energy

transfer between T and $T + dT$ is

$$dP = N\Delta R\sigma(E,T)dT. \tag{3}$$

Then the energy loss of the particle is given as

$$\Delta E = \int T dP = N\Delta R \int T\sigma(E,T)dT. \tag{4}$$

For infinitesimal ΔR, this leads to a definition of stopping cross-section $\sigma_S(E)$

$$\sigma_S(E) = \int T\sigma(E,T)dT, \tag{5}$$

which multiplied with N gives the average stopping power.

The cross section σ can be determined for any type of energy transfer (nuclear, electronic, charge transfer etc.) and the total energy loss is then calculated by summing up these contributions.

The analytical models for nuclear stopping of ions constitute the two-body scattering problem [5]. In a basic elastic scattering of two charged particles, the energy transferred from one particle to another can be easily derived using conservation of energy and momentum. The scattering is governed by a basic quantity: the nearest distance from the original ion trajectory to the atom, which is called the impact parameter p. The calculation of the energy loss using eq. 5 is complicated due to the electron clouds screening the two nuclei. It can be done by choosing a spherically symmetric screening function. The interaction potential is obtained as a product of the screening function and the Coulombic term. There are many different formulations of the screening function [33] and one of the most used is the universal screening function by Ziegler, Biersack and Littmark (ZBL) [5]. Using an appropriate screening function, the nuclear stopping of any ion in any target material can be evaluated analytically [6].

Analytical models for the electronic stopping have been traditionally divided into the three velocity regimes. Early models of the stopping of a fast ($v > v_0$) heavy ion date back to Bohr (see e.g. ref. [34]) who calculated the problem of electron scattering from the moving ion and calculated a semi-classical limit for the stopping cross section of a fast ion. A quantum mechanical model by Bethe (see e.g. [35, 36]) is commonly used for a fully stripped ion, i.e. when $v > 2Z_1 v_o$, which is the limit of the transition to the classical regime governed by Bohr's formula. Bethe's model and the correction terms from the shell-corrections [25, 37], Bloch correction [38], the polarization effect [28] (or Barkas

effect or Z_1^3 contribution), and relativistic effects [39] give an accurate and extensively used analytical description of the stopping of fast ions.

The first general model for the nuclear and electronic stopping of an ion was presented by Lindhard *et al.* [10, 40], who based their treatment of atoms on the statistical atomic model of Thomas and Fermi. The LSS model gives analytical formulae for the nuclear and the electronic stopping of any ion in any target material in the low-velocity region. The LSS theory gave a basis for the description of the different velocity regions. The LSS theory has been found to give a good mean description of the stopping of heavy ions, while neglecting the Z_1 and Z_2 -oscillations.

In modern electronic stopping calculations, the electron-gas models are in an important position. The target is treated as an electron gas (or plasma) with a constant density ρ and the ion is seen as a perturbation in the gas [5]. The semi-classical analysis of the perturbation model uses Poisson's equation for a charge interacting with a polarizable medium characterized by the dielectric function [6]. The stopping integrals in the dielectric formalism [41] can be calculated using Lindhard's linear approximations for the dielectric function both for the slow and the fast ions. An inhomogeneous electron density of the target can be treated with the Local Density Approximation (LDA), in which each unit volume of the plasma is considered to be homogeneous plasma and by applying Lindhard's interaction function to the ion, the stopping is integrated over the volume of the ion. More advanced nonlinear calculations using Feynman diagrams and Density Functional Methods by Ritchie, Ferrell, Echenique and Nieminen [19, 42] gave good results for metallic densities.

In the intermediate velocity region, the analytical models have typically interpolated between the Bethe formula above the stopping maximum and linear models below the stopping maximum. One of the most important improvements in this region was the BK-model by Brandt and Kitagawa [43], which gave a simple connection between the ionization of the heavy ion and its stopping power. The BK-model implicitly contains the idea that the energy loss increases for small impact parameters due to reduced screening. The electronic stopping of a heavy ion in the BK-theory is factorized into the effective charge of the ion Z_{eff} and the electronic stopping of a proton S_p as

$$S_e = Z_{eff}^2 S_p, \tag{6}$$

where

$$Z_{eff} = \gamma Z_1. \tag{7}$$

The theory contains the Fermi velocity of the target electrons, fractional ionization of the ion γ, which is determined from the velocity of the ion relative to the electrons, and the screening length for the ion.

The stopping calculations on the basis of BK-theory were improved in the ZBL-parametrization, which is a nonlocal model for calculating heavy ion stopping in the whole velocity region up to relativistic velocities. A large amount of experimental data was used for parametrizing the ionization degree γ and the screening length of the ion. Using the scaling law in eq. 6, the ZBL-parametrization gives the empirical stopping of any ion in any target material. The Fermi velocity in this parametrization is a constant value for each target material, so the ion velocity and the atomic numbers remain the only parameters for the stopping function. Due to the several fitted parameters, the predicted electronic stopping powers are reasonably accurate [44] but the non-locality makes it useless for stopping calculations in crystals, where channeling is important.

A common feature to all the analytical models for velocities below or near stopping maximum is that the theoretical prediction can differ several tens of percent from the experimentally measured values. Recent models attempting to improve the accuracy in the stopping calculations using numerical methods are the Binary-Theory [26] and the generalization of the Friedel sum rule [24, 33, 45, 46] for non-crystalline targets, and the convolution approximation [47–49] for crystalline targets.

Analytical models of particle penetration rely on the use of statistical physics methods and transport equations [50] for the slowing down of an ion in a homogeneous, non-correlated (successive collisions are statistically independent) environment. These equations can be solved only for a limited set of environments and thus computer simulations have become widely used.

4.2 MC models

The analytical calculations can be used to deduce the stopping power as a function of the ion velocity and impact parameter. Range profiles of ions implanted into a material are obtained in computer simulations of ion movements inside materials. The implantation of ions is simulated by following the ions' penetrations until they stop and a histogram of the penetration depths from the target surface is used to give the range profile of the ions.

One of the main tools in the field of statistical particle penetration has been the use of transport equations and Monte Carlo (MC) techniques to solve them numerically [6]. In fact, particle penetration has been one of the first major applications of computer simulations in physics [6].

In the MC technique, the ion movement is simulated as follows. A random number generator is used to determine the free flight path l (or one can use a fixed mean free path) of an ion from an exponential distribution $F(l)$

$$F(l) = \frac{1}{\lambda} e^{-\frac{l}{\lambda}}, \tag{8}$$

where $\lambda = 1/(N\sigma(E))$ is the mean free path, N is the atom density of the target and $\sigma(E)$ is the total cross-section, i.e. the cross section for all possible collisions under consideration. Then the type of a collision is randomly determined resulting in a new direction, charge state, energy etc. for the ion. Each collision is treated as binary, and the rest of the environment is neglected. This procedure is then iterated until the ion has lost all of its energy.

Computer models that treat the successive collisions as binary are called Binary-Collision-Approximation (BCA) [51] models. These models are basically MC models. BCA models that are capable of treating crystalline structures are called crystal BCA or lattice BCA models. The key quantity in all the BCA models is the impact parameter of the ion, which determines the energetics of the collision.

The idea of individual binary collisions breaks down for low ion energies [52] and the electron structure of the target is usually not treated properly, since the charge distributions in a crystal structure are not spherically symmetric around the nuclei. There is a way for taking into account a realistic electron distribution of the Si crystal in BCA models, but the calculation method must be completely rewritten to evaluate the ion's trajectory more carefully [53].

The MC calculation is very fast with modern computers, with simulation times of only seconds or minutes. There are several BCA-codes [54–57] available of which the code most used is TRIM [56]. A common problem with the BCA codes is the use of free parameters needed to select the next colliding ion, which do not always have a physical meaning.

4.3 MD models

In the Molecular Dynamics (MD) simulation method, the movement of the ion is followed more accurately than in the BCA methods. Two factors contribute to this: firstly the properties of the target structure can be described more realistically and secondly the ion can interact with several atoms at a time.

In MD simulations, the atoms in the system are given initial space and momentum coordinates. By solving the Newtonian equations of motion in a small time-step for all the atoms, the atom coordinates

are changed. This process is then iterated until the given criteria (for example the maximum time) for the ending of the simulation is fulfilled. The accuracy of the ion movement depends on the length of the time step, but using a sufficiently short time step the solution can be made accurate.

The movement of the atoms is determined by the forces interacting between them. These forces depend on the interaction potentials of the atoms, which are usually divided into repulsive and attractive parts. The repulsive part is the most important in the range calculations and can be written as a screened Coulomb interaction

$$V(r) = \frac{Z_1 Z_2 e^2}{r^2}\Phi(r), \tag{9}$$

where $\Phi(r)$ is the screening function. There are several attempts to universally describe how the electrons screen the nucleus [6], of which the universal ZBL repulsive function is the most used one. It is achieved by fitting a function to a large set of theoretically calculated pair potentials and in individual cases it can have a margin of error of about ten percent [5]. The repulsive potentials used in this thesis are calculated with the DMol package [58], which uses DFT methods for self-consistent calculation of the dimer potential. It has been found that the DMol calculations produce potentials with an accuracy of 1 % compared to highly accurate Hartree-Fock calculations [59].

The electronic stopping of an ion in MD simulations is taken into account as a drag force acting on the moving ion. This force is calculated with the chosen electronic stopping model.

The MD method makes it possible to include all the many-body-collisions neglected in the BCA simulations. Thus it is the only way to calculate ion movement for low energies or in case of cluster implants. The electronic structure of the target material can also be constructed accurately because the space coordinates of all atoms in the simulation are determined during every time step. A full MD simulation is very time-consuming and this limits its use to very low-energies ($<$ 1 keV/amu), even when supercomputers are used.

The concentration of doped atom species varies several decades in a typical range profile of interest. This means at least 1000-10000 simulations of ion implantation events for each profile, making the use of full MD impossible. There are, however, approximations that can be used for the simulation of range profiles. These are listed below:

1. Only the repulsive potentials are used for the atoms.

2. Only the interaction between the projectile and the atoms are calculated. This is called the Recoil Interaction Approximation (RIA).

3. The interactions are calculated only in a small environment (simulation cell) surrounding the moving ion. For periodic structures this is simple.

4. The ions are divided into virtual ions in areas of low concentration to keep the statistics at the same level for each concentration level. This is called the Rare Event Enhanced Domain-algorithm (REED) [60].

5. A variable time step is used.

Using these approximations, the maximum simulation time is only minutes or hours with normal desktop computers, thus approaching the efficiency of BCA codes. The MD code developed in our laboratory for calculating range profiles using the above-mentioned approximations is called MDRANGE [61, 62] and it is the basis for all range calculations done in this thesis, except those for clusters in paper III. The downside of the approximation used is that the cascades are neglected, which means that the change in the target structure can not be calculated directly.

5 ELECTRONIC STOPPING IN CHANNELS

The silicon crystal is formed from periodic diamond-structured cells, in which the atoms are covalently bonded. The periodicity in the structure forms channels into silicon, and for the ion moving in the channel, not only is the atom density lower but the electron density is several decades lower than near the nucleus. This has a pronounced effect of decreasing the stopping power, both nuclear and electronic, of an ion moving in the channel compared to the movement in a random direction. Atomic units ($m = e = \hbar = 1$) are used throughout this chapter.

5.1 Simulation models for low-energy stopping in channels

Two different approaches are used to calculate the electronic stopping: BCA-models which use the impact parameter and MD-models which use the local electron density as the key variable. The benefit of the impact parameter models is that the different stopping contributions are better separated using cross sections and theoretically easier to calculate. The MD models benefit from the possibility of knowing the precalculated local electron density accurately inside the material and the possibility of having many-body-collisions. We use an MD model with the local electron density approach.

In electron gas theories, the lower electron density in the channels decreases the electronic stopping of an ion simply because there are fewer electrons to collide with. The electrons in the channel are

either free (metals) or nearly free valence electrons (semiconductors). Thus the contribution to the stopping from the bound electrons is less important in channels.

Channeling stopping powers have been calculated in MD simulations using models based on the BK-theory. The model by Beardmore, Grønbech-Jensen and their co-workers (BGJ) [60, 63] uses spherical charge densities for the target atoms, which are used as the local information in their model. The stopping power is calculated using eq. 6 and an improved linear response theory for the stopping of the protons. The effective charge of an ion is calculated using a *fitted* Fermi velocity for the material, which is the only free parameter in the BGJ-model. Due to the fitting their model gives very good results for the low-energy channeling of ions.

Sillanpää *et al.* developed a model [17] based on the BGJ-model, in which they used a more accurate three-dimensional electron density distribution for crystalline silicon to give the local electron density n **and** the local Fermi velocity inside the crystal. The Fermi velocity is related to the one-electron radius as:

$$v_F = \frac{1}{\alpha r_s}, \tag{10}$$

where $r_s = [3/(4\pi n)]^{1/3}$ and $\alpha = [4/(9\pi)]^{1/3}$.

5.2 Electronic stopping for slow ions

Our model [I,II,IV,V] is developed from the model by Sillanpää. We do not calculate the stopping of a proton and use scaling for the heavier ions, but we calculate the stopping of a heavy ion directly. The electronic stopping of a slow ion can be calculated with the non-linear free-electron-gas model [19] as:

$$S_{free}(v) = v v_F n \sigma_{tr}(v_F) = \frac{3v}{k_F r_s^3} \sum_{l=0}^{\infty} (l+1) \sin^2(\delta_l(E_F) - \delta_{l+1}(E_F)), \tag{11}$$

where v is the ion velocity, k_F is the Fermi wave number, n is the electron density, $r_s = (4\pi n/3)^{-1/3}$ is the one-electron-radius and $\delta_l(E_F)$ are the phase-shift values for an electron scattering from the Fermi surface. This is the limit of a static case for the spherically symmetric scattering potential [40]. The phase shift values for a given ion are precalculated with Density Functional Theory (DFT) [64] for a grid of electron density values ranging from $r_s = 0.1$ to $r_s = 6.0$ in atomic units. This gives us

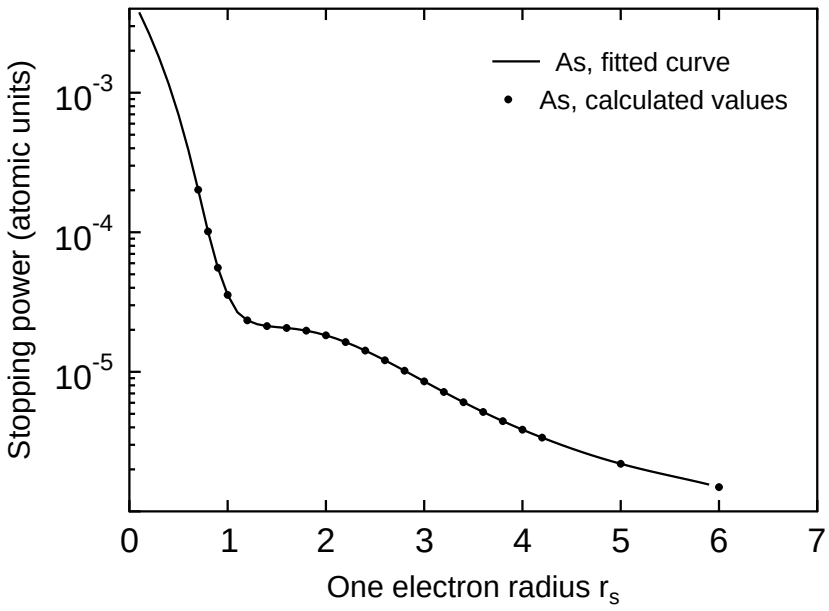

Figure 8: DFT results of free-electron-gas (one-electron-radius r_s) stopping of As ions calculated using eq. 11.

the value of the sum in eq. 11 as a function of electron density. Figure 8 shows an example of the precalculated values and the interpolated function.

To calculate the stopping of a moving ion in our MD simulations using the results of the DFT calculation, we need the electron number density n at the position of the ion, which gives us also r_s and k_F. The three-dimensional charge distribution is calculated for a crystalline Si unit cell using the Dawson-Stewart-Coppens formalism [65, 66] and the Hartree-Fock wave functions calculated by Clementi and Roetti [67]. While the atom is moving inside the silicon, we get the desired electron density from the 3D distribution in the given location inside the unit cell. This means that our electronic stopping model is local. The 3D-distribution table can be calculated either for the total electron density or for the valence electron density only. We used the total electron density and eq. 11 in the calculations in paper I. In this context the electron density can be thought of as an effective electron density governing both the free-electron-gas stopping and the electron exchange processes in close collisions. Although not physically rigorously well motivated, this often works surprisingly well (see fig. 10).

In paper V, we took the better motivated approach of using only the valence electron density in eq. 11. We also needed a theory for the during-the-collision electronic stopping by Firsov, because eq. 11 accounts only for the free-electon-gas energy loss between the close collisons. The approach derived

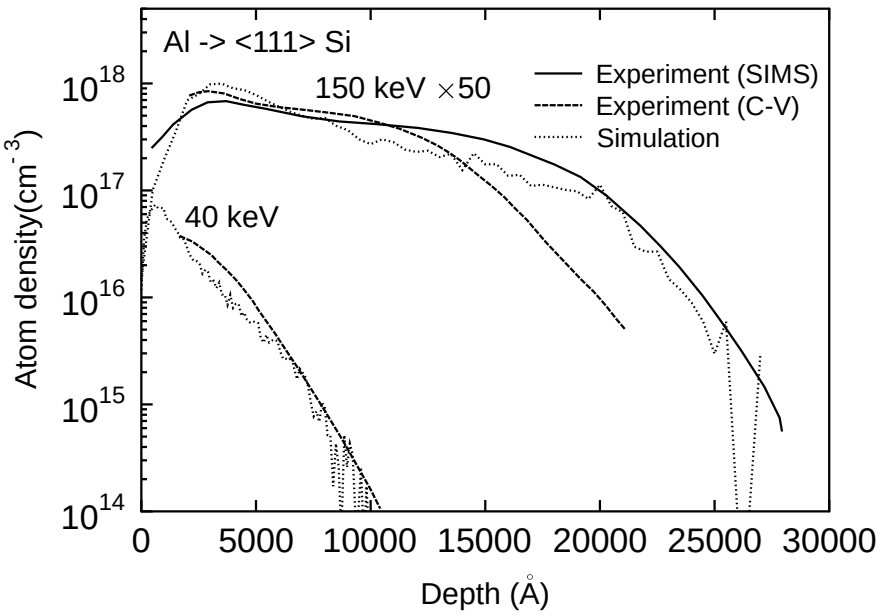

Figure 9: Simulated [I] and experimental [68, 69] range profiles of Al ions implanted in the <111> channeling direction in Si. The simulation used the total electron density of silicon and eq. 11 to calculate the electronic stopping power of Al ions. The atom density in the 150 keV profiles are multiplied by 50 to clarify the picture.

by Elteckov *et al.* [70] based on Firsov's theory gives the force due to inelastic interactions when the ion is close to the atom as

$$F(R,v) = \frac{-0.7h}{(\pi a_0)^2}\left[\frac{Z_A^2}{(1+0.8dZ_A^{1/3}R/a)^4} + \frac{Z_B^2}{(1+0.8(1-d)Z_B^{1/3}R/a)^4}\right]v \text{ N}, \tag{12}$$

where Z_A and Z_B ($Z_A > Z_B$) are the atomic numbers of the colliding atoms, a_0 is the Bohr radius, $a = 0.47\text{Å}$ and d = 1 / [1 + $(Z_B/Z_A)^{1/6}$]. The range of validity of Firsov's formula is limited to cases when max(Z_i/Z_j)<4. This method was used in paper V with good results (fig. 11) for all ions for which experimental data was available.

There is a problem in the assumption that the ion is thought of as point-like in the MD simulations. Ions moving in the most open channel in silicon, the <110> channel, can experience extremely low electron densities and thus penetrate long distances in the channel. This can be taken into account by

using a correction term for raising the very lowest electron densities. This addition of a free parameter reduces the ranges dramatically in the <110> channel but does not affect the range profiles in other directions [V].

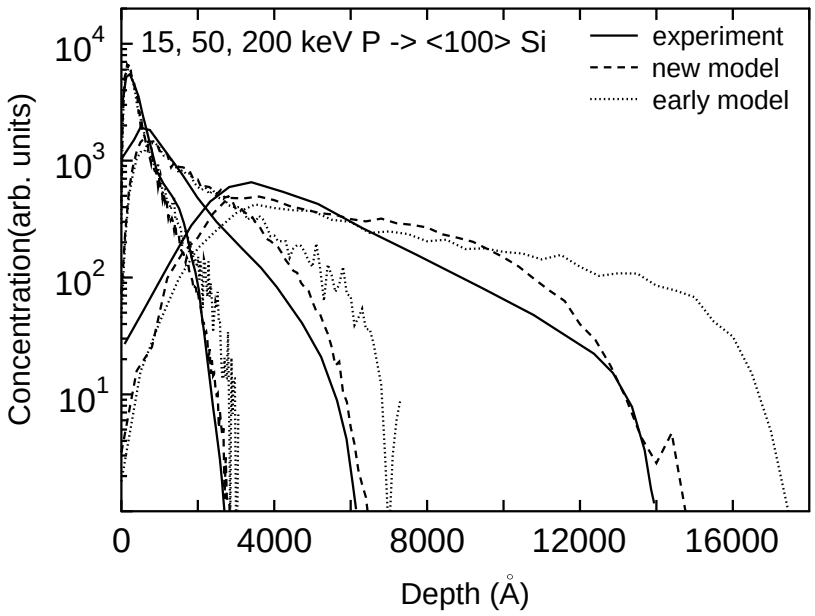

Figure 10: Simulated and measured (SIMS [68, 71]) ranges of 15, 50 and 200 keV P ions in the <100> channel of Si. The early model [I] uses total electron density and eq. 11 to account for the electronic stopping. The new model [V] uses valence electron density in eq. 11 together with a Firsov's model for taking into account the electronic stopping during close collisions between the ion and the atoms.

5.3 Extension to swift ions

For the fast ions, the static case approximation obviously breaks down and eq. 11 can not be used. Physically the reason is that the induced potential of a moving ion differs from the spherically symmetric case, making the normal assumptions for the transport cross-section and the numerical solving of the Schrödinger equation not valid. Salin *et al.* have performed a fully non-linear calculation [72], taking into account the cylinderical symmetry of the potential at finite velocities, and their calculations show that the linearity in the velocity holds up to the Fermi velocity. Another way of expanding the velocity range of the stopping calculation is to use a spherically symmetric approximation of the moving cylinderically symmetric potential. Lifschitz and Arista have formulated a model [24, 45] for calculating the electronic stopping of a moving ion using a velocity dependent screening parameter for the spherical average potential. The screening parameter is self-consistently adjusted so that the

Extended Friedel Sum Rule (EFSR) [45] is fulfilled for the phase shifts which result from the numerical solving of the Schrödinger equation for the spherical potential. Because the charge state of the ion is a function of velocity, the stopping power must be calculated for each possible charge state i separately and the contributions summed as

$$S_{tot} = \sum_i \Phi_i(v) S_i, \tag{13}$$

where $\Phi_i(v)$ are the equilibrium charge state fractions. This formulation takes into account only the free-electron gas contribution to the stopping power, so other theories must be used for taking into account the contributions from other relevant processes. In the channeling case, the importance of the other contributions is minimized.

We have used the above formulation for calculating channeling stopping powers for He ions in Si up to an energy of 3 MeV [VI]. Due to the uncertainties arising from the requirement of knowing the charge state fractions in this formulation, we have also developed an interpolation scheme for the stopping power calculation. Knowing the linear low velocity stopping presented in eq. 11 and the Bethe formulation [28]

$$S_{Bethe}(v) = \frac{Z_1^2 \omega_P^2}{v^2} ln(\frac{2v^2}{\omega_P^2}) \tag{14}$$

for the high velocity stopping, where $\omega_P^2 = \sqrt{4\pi n}$ is the classical plasma frequency, we can use quadratic interpolation of these two to get a stopping formulation for the intermediate velocities. Using the interpolation scheme we can eliminate the calculation of different charge state fractions, and our results show that for the He ions, the interpolation scheme gives approximately the same results as the charge state fraction calculation. We also calculated the channeling stopping powers for Li and O. The calculations showed a decent agreement for the Li stopping compared to the experiments and revealed that the O ions were too heavy for the stopping to be modeled with a simple interpolation.

5.4 Effect of high dose on channeling

If the implantation fluence ($ions/cm^2$) is high enough, the probability that an ion hits a surface area that has been damaged by the previously implanted ions increases. Thus the range profile of ions can not be calculated assuming the same target structure for all ions in the simulations. The originally perfect crystal becomes damaged and its channels are blocked when implanted ions break the bonds in the crystal. The amount and the persistence of the damage depends on the ion flux, implantation fluence and the atom types. The most noticeable effect is the blocking of the channels, which is

clearly seen as a reduction of the channeling tail of the range profile (fig. 11). There are many BCA codes designed to handle this eventuality. They typically use fitted probabilities for atom displacement and recombination processes [73, 74]. In the MD simulations, the damage build-up process can be described by changing the atom positions in the crystal as the energy deposited into it by the ions increases. We have calculated the deposited nuclear energy of ions in silicon as a function of depth [II]. By knowing the ion fluence, we can calculate to how many real ions one simulated ion corresponds and determine how much energy it deposits into the crystal for a given fluence. The atom positions are changed during the simulation according to the predamaged crystal cells, which have different degrees of damage as a function of the deposited energy. The damaged crystal cells are taken from a full MD simulation of radiation damage [29]. The downside of this procedure is that the type of the ion does not affect the type of damage, which is an important effect because the fraction of damage in clusters depends on the ion species and affects the range profile [75]. Nevertheless, even our simpler model reproduces a wide range of Si implant conditions well [II] (see fig. 12).

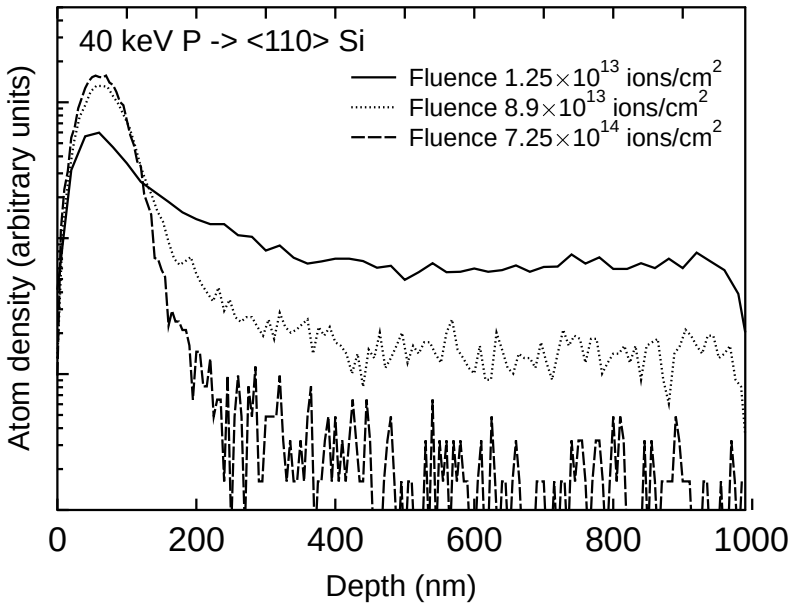

Figure 11: Effect of the damage build-up on the simulated channeling (<110>) direction implantation profiles of 40 keV P. The profiles are scaled to the same area.

6 NUCLEAR STOPPING OF ATOM CLUSTERS

When implanting atoms in the form of clusters or molecules [30] containing 2-10000 atoms, the implantation energy per atom can be decreased and the beam divergence can be better controlled

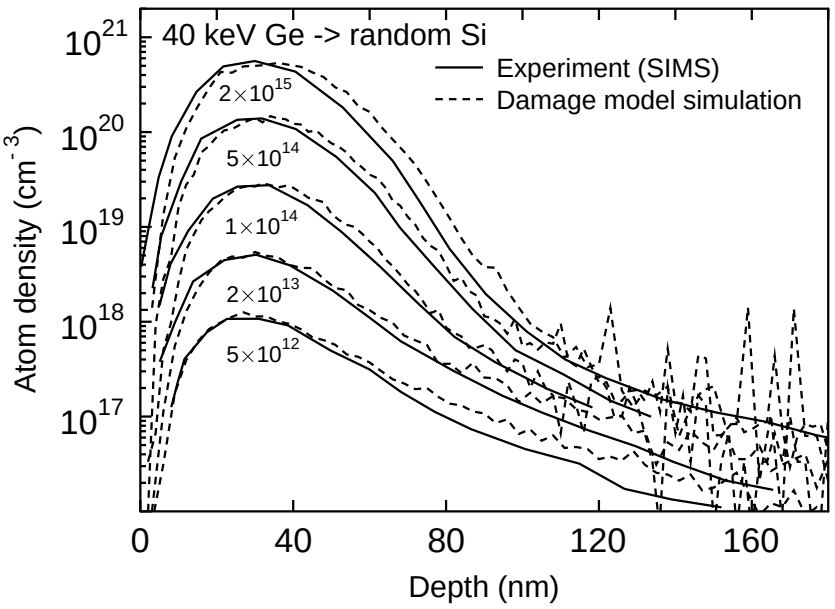

Figure 12: Simulated [II] and experimental [76] range profiles of 40 keV Ge ions implanted in a "random" direction in Si with various fluences ($ions/cm^2$). The simulations are done using the damage build-up model.

for low energy implantations. This is important because the semiconductor industry needs smaller transistor sizes which require lower implantation energies.

In a cluster bombardment, a high energy density is deposited in a small area of the surface. The implanted clusters can either create a massive eruption of surface atoms creating craters [77], or they can land gently on the surface creating nanohillocs [78]. Clusters can also spread on the surface, decreasing the surface roughness, or they can be used in shallow junction formation as dopants [79, 80]. The physics of cluster beams is primarily dependent on the atom types and implantation energy.

6.1 Stopping of a cluster

Theoretical understanding of a cluster impact is more difficult than of ion impacts due to the nonlinear effects arising from the interaction between the cluster atoms [81–84]. The stopping of a cluster of n atoms is not necessarily n times the stopping of one individual ion. The difference is usually called the *vicinage effect*. From the electronic stopping point of view, the difference has been explained as originating from the interference in the electronic excitations of the target due to the correlated motion

of the penetrating ion. This has been found to enhance the stopping of a cluster in certain conditions [6].

There are also experimental [7] and theoretical [81] findings that the nuclear stopping power of an atom in a cluster is less than the nuclear stopping of a single ion. One proposal has been the clearing-the-way effect, in which the reduction is explained to be caused by the clearing of the target atoms by the front atoms in the clusters, thus making the lattice more open to the atoms belonging to the same cluster behind them.

The definition of the stopping of a cluster is not always clear, because the cluster can break down into single ions before the ions stop penetrating the target.

6.2 Low-energy Au_n (n=1-7) clusters in Cu and Si

To examine the nonlinearities of cluster impacts, we have simulated the implantation of small gold clusters with energies of 1 - 10 keV/atom in the non-channeling direction of Cu and Si [III]. The results show that the clusters break down into single ions on the surface and those ions continue penetrating the material as individual ions. This brings the average penetration depth (mean range) near the case of individual impacts, but the large liquid volume created by the cluster impact in Cu spreads the stopped ions (Fig. 13), greatly increasing the straggling in the range profile. This does not happen in Si, because of the lack of heat spikes in silicon due to the more open nature of its lattice structure [85, 86]. The simulation results of the heat spike effect are in agreement with the experiments done by Andersen [7], which were the motivation for the study in paper III. The mean range in Cu also increases in the simulations as the cluster size increases, because the stopping power of the atoms in a cluster is found to be less than that of the single ions. This clearly supports the idea of the clearing-the-way effect.

7 CONCLUSIONS

We have studied the use of the free-electron-gas electronic stopping power calculation in the framework of MD simulations in several different schemes. Using the DFT code, we have calculated the response of the electron gas to a heavy ion in a range of electron densities. This was used to calculate the electronic stopping of a slow ion in crystalline silicon using an accurate 3D charge distribution. In non-crystalline silicon and GaAs we used spherically symmetric charge distributions. The same stopping calculation was used in a study of the damage accumulation processes in c-Si. Extension to

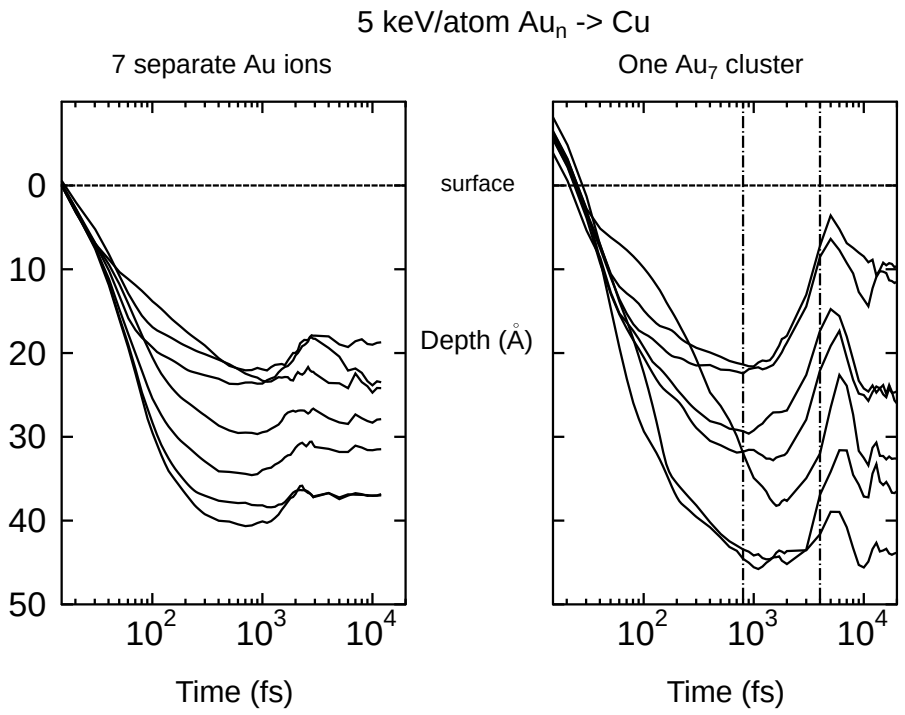

Figure 13: Different penetration behavior of individual impacts and a cluster impact in Cu. The picture on the left hand side shows the depth trajectories of 7 single Au ions implanted separately into Cu in individual simulations. The picture on the right hand side shows the same for a cluster consisting of 7 Au atoms. The heat spike time interval, during which the ions spread apart, is marked with dashed lines.

swift light ions was studied by changing the DFT calculations to a standard numerical procedure for the solving of the response of the electron gas to a moving spherically symmetrical average potential. None of these methods involve free parameters, which can be considered to be a guide line of this thesis. The simulated range profiles of low energy ions in silicon and GaAs show in most cases excellent agreement with the experimental results both for the non-destructive and damage accumulation cases. The stopping calculations for the swift light ions show promise for extending the MD calculations to higher energies. The <110> channel is a special case in the simulations due to the extremely low electron densities experienced by the point-like ions and needs further improvement in the simulation method, which was partly done in paper V. The stopping and the kinematics of small Au cluster implants in Cu were studied and the reason for the experimentally observed increase in the straggling of the range profile was found to be the atomic mixing in the heat spike.

ACKNOWLEDGEMENTS

This study was carried out at the Accelerator Laboratory between the years 2000 and 2003. I wish to thank the former and current heads of the laboratory, Doc. Eero Rauhala and Prof. Jyrki Räisänen, for placing the facilities of the laboratory at my disposal.

I am grateful to my co-supervisor, Prof. Juhani Keinonen, the head of the Department of Physical sciences, for his guidance and valuable discussions.

Special thanks are due to my supervisor Prof. Kai Nordlund, who had a major part in tutoring me through my short scientific career. Without Kai, the making of this thesis would not have been possible.

I also wish to thank all my colleagues at the Accelerator Laboratory for the informative discussions and warm working atmosphere, especially J. Nord, J. Tarus, E. Salonen and J. Franz.

I want to thank my Mother and Father for the support and guidance over the years, my sister and finally, my own family Anu and Tuuli for being there.

Financial support from the Academy of Finland, the Vilho, Yrjö ja Kalle Väisälä and Magnus Ehrnrooth foundations is gratefully acknowledged.

Helsinki, June 2003
Jarkko Peltola

REFERENCES

1. *Materials science and engineering, 5th edition*, edited by W. D. Callister (John Wiley and Sons, US, 2002).

2. *Optical effects of ion implantation*, edited by P. D. Townsen, P. J. Chandler, and L. Zhang (Cambridge university press, Great Britain, 1994).

3. *Handbook of modern ion beam analysis*, edited by J. Termer, M. Nastasi, J. Barbour, C. Maggiore, and J. Meyer (Materials research society, Pittsburg, 1995).

4. N. Bohr, Phil. Mag. **25**, 16 (1913).

5. J. F. Ziegler, J. P. Biersack, and U. Littmark, *The Stopping and Range of Ions in Matter* (Pergamon, New York, 1985).

6. *Interaction of charged particles with solids and surfaces*, edited by A. Gras-Marti, H. M. Urbassek, N. Arista, and F. Flores (Plenum Press, New York, 1991).

7. H. H. Andersen, A. Johansen, M. Olsen, and V. Touboltsev, *Gold-cluster ranges in aluminium, silicon and copper*, Nucl. Instr. Meth. Phys. Res. B (2003).

8. P. Sigmund, *Stopping power in perspective*, Nucl. Instr. Meth. Phys. Res. B **135**, 1 (1998).

9. *Fundamentals of semiconductors, 2nd edition*, edited by P. Y. Yu and M. Cardona (Springer-Verlag, Germany, 1999).

10. J. Lindhard, M. Scharff, and H. E. Shiøtt, *Range concepts and heavy ion ranges*, Mat. Fys. Medd. Dan. Vid. Selsk. **33**, 1 (1963).

11. *Ion implantation*, edited by G. Dearnaley, J. H. Freeman, R. S. Nelson, and J. Stephen (North-Holland publishing company, Amsterdam, 1973).

12. K. S. amd C. Trautmann and R. Neumann, *Electronic excitations and heavy-ion-induced processes in ionic crystals*, Nucl. Instr. Meth. Phys. Res. B **209**, 73 (2003).

13. E. Fermi and E. Teller, *The capture of negative mesotrons in matter*, Phys. Rev. **72**, 399 (1947).

14. R. H. Ritchie, *Interaction of charged particles with degenerate Fermi-Dirac electron gas*, Phys. Rev. **114**, 644 (1959).

15. L. G. Glazov, *Frozen-charge stopping of ions in the Bethe regime*, Nucl. Instr. Meth. Phys. Res. B **195**, 118 (2002).

16. *Case studies in atomic collision physics I*, edited by E. W. McDaniel and M. R. C. Mcdowell (North-Holland publishing company, Amsterdam, 1969).

17. J. Sillanpää, K. Nordlund, and J. Keinonen, *Electronic stopping of Silicon from a 3D Charge Distribution*, Phys. Rev. B **62**, 3109 (2000).

18. P. Sigmund, A. Fettouhi, and A. Schinner, *Material dependence of electronic stopping*, Nucl. Instr. Meth. Phys. Res. B **209**, 19 (2003).

19. P. M. Echenique, R. M. Nieminen, J. C. Ashley, and R. H. Ritchie, *Nonlinear stopping power of an electron gas for slow ions*, Phys. Rev. A **33**, 897 (1986).

20. I. Nagy, A. Arnau, and P. M. Echenique, *Nonlinear stopping power and energy-loss straggling of an interacting electron gas for slow ions*, Phys. Rev. A **40**, 987 (1989).

21. K. Shima, N. Kuno, and M. Yamanouchi, *Z_1 and Z_2 oscillation of mean charges of ions (energy appr. 1 MeV/u) emerging from a thin foil*, Chinese journal of physics **26**, 292 (1988).

22. G. de M. Azevedo, M. Behar, and P. L. Grande, *Range study of Eu implanted into Si channeling directions: Evidence for the Z_1 effect*, Phys. Rev. B **63**, 64101 (2001).

23. Reprinted from Nucl. Instr. Meth. Phys. Res. B, 195, P. Sigmund and A. Schinner, Binary theory of electronic stopping, 64, Copyright (2002), with permission from Elsevier.

24. A. F. Lifschitz and N. R. Arista, *Electronic energy loss of helium ions in aluminum using the extended-sum-rule method*, Phys. Rev. A **58**, 2168 (1998).

25. J. R. Sabin and J. Oddershede, *Shell corrections to electronic stopping powers from orbital mean excitation energies*, Phys. Rev. A **26**, 3209 (1982).

26. P. Sigmund and A. Schinner, *Binary theory of electronic stopping*, Nucl. Instr. Meth. Phys. Res. B **195**, 64 (2002).

27. J. Sillanpää, *Phenomenological model for electronic stopping of low-velocity ions in crystalline solids*, Report series in physics: HU-P-D84 **84**, 1 (2000), PhD thesis, University of Helsinki.

28. J. M. Pitarke, R. H. Ritchie, and P. M. Echenique, *Quadratic response theory of the energy loss of charged particles in an electron gas*, Phys. Rev. B **52**, 13883 (1995).

29. J. Nord, K. Nordlund, and J. Keinonen, *Amorphization mechanism and defect structures in ion beam amorphized Si, Ge and GaAs*, Phys. Rev. B **65**, 165329 (2002).

30. *Ion implantation in semiconductors*, edited by I. Ruge and J. Graul (Springer-Verlag, Berlin, 1971).

31. S. Tian, *Predictive Monte Carlo ion implantation simulator from sub-keV to above 10 MeV*, J. Appl. Phys. **93**, 5893 (2003).

32. C. Park, K. Klein, A. Tasch, and J. Ziegler, *Critical angles for channeling of boron ions implanted into single-crystal silicon*, J. Electrochem. Soc. **138**, 2107 (1991).

33. N. R. Arista, *Energy loss of ions in solids: Non-linear calculations for slow and swift ions*, Nucl. Instr. Meth. Phys. Res. B **195**, 91 (2002).

34. P. Sigmund and A. Schinner, *Binary stopping theory for swift heavy ions*, Eur. Phys. J. D. **12**, 425 (2000).

35. P. Sigmund and A. Schinner, *Effective charge and related/unrelated quantities in heavy-ion stopping*, Nucl. Instr. Meth. Phys. Res. B **174**, 535 (2001).

36. P. Sigmund and A. Schinner, *Binary theory of antiproton stopping*, Eur. Phys. J. D. **15**, 165 (2001).

37. J. R. Sabin and J. Oddershede, At. Data Nucl. Data Tab. **31**, 275 (1984).

38. H. Bichsel, *Shell corrections in stopping powers*, Phys. Rev. A **65**, 52709 (2002).

39. E. Uggerhøj, *Some energy-loss and channeling phenomena for GeV particles*, Physica Scripa **28**, 331 (1983).

40. P. M. Echenique, I. Nagy, and A. Arnau, *Interaction of slow ions with matter*, Int. J. of Quantum Chem. **23**, 521 (1989).

41. D. G. Arbo and J. E. Miraglia, *Collisional stopping considering the induced potential created by ions in a free-electron gas*, Phys. Rev. A **58**, 2970 (1998).

42. T. L. Ferrell and R. H. Ritchie, *Energy losses by slow ions and atoms to electronic excitation in solids*, Phys. Rev. B **16**, 115 (1977).

43. W. Brandt and M. Kitagawa, *Effective stopping-power charges of swift ions in condensed matter*, Phys. Rev. B **25**, 5631 (1982).

44. H. Paul and A. Schinner, *An empirical approach to the stopping power of solids and gases for ions from Li to Ar*, Nucl. Instr. Meth. Phys. Res. B **179**, 299 (2001).

45. A. F. Lifschitz and N. R. Arista, *Velocity dependent screening in metals*, Phys. Rev. A **57**, 200 (1998).

46. N. R. Arista, *Erratum: Energy loss of ions in solids: Non-linear calculations for slow and swift ions [Nucl. Instr. and Meth. B 195 (2002) 91-105]*, Nucl. Instr. Meth. Phys. Res. B **207**, (2003).

47. P. L. Grande and G. Schiwietz, *Impact-parameter dependence of the electronic energy loss of fast ions*, Phys. Rev. B **58**, 3796 (1998).

48. G. Schiwietz and P. L. Grande, *A unitary convolution approximation for the impact-parameter dependent electronic energy loss*, Nucl. Instr. Meth. Phys. Res. B **153**, 1 (1999).

49. G. de M. Azevado, P. L. Grande, and G. Schiwietz, *Impact-parameter dependent energy loss of screened ions*, Nucl. Instr. Meth. Phys. Res. B **164**, 164 (2000).

50. P. Sigmund, *LSS and the integral equations of transport theory*, Physica Scripta **28**, 257 (1983).

51. M. T. Robinson and I. M. Torrens, *Computer Simulation of atomic-displacement cascades in solids in the binary-collision approximation*, Phys. Rev. B **9**, 5008 (1974).

52. G. Hobler and G. Betz, *On the useful range of application of molecular dynamics simulations in the recoil interaction approximation*, Nucl. Instr. Meth. Phys. Res. B **180**, 203 (2001).

53. J. M. Hernandez-Mangas, J. Arias, L. Bailon, M. Jaraiz, and J. Barbolla, *Improved binary collision approximation ion implant simulators*, J. Appl. Phys. **91**, 658 (2002).

54. M. T. Robinson, *Computer simulation studies of high-energy collision cascades*, Nucl. Instr. Meth. Phys. Res. B **67**, 396 (1992).

55. M. Hautala and I. Koponen, *Distributions of implanted ions in solids*, Defect and Diffusion Forum **57-58**, 61 (1988).

56. J. P. Biersack and L. G. Haggmark, *A Monte Carlo computer program for the transport of energetic ions in amorphous targets*, Nucl. Instr. Meth. **174**, 257 (1980).

57. W. Möller and W. Eckstein, *TRIDYN - a TRIM simulation code including dynamic composition changes*, Nucl. Instr. Meth. Phys. Res. B **2**, 814 (1984).

58. DMol is a trademark of Bio Sym. Inc., San Diego, California, USA.

59. K. Nordlund, N. Runeberg, and D. Sundholm, *Repulsive interatomic potentials calculated using Hartree-Fock and density-functional theory methods*, Nucl. Instr. Meth. Phys. Res. B **132**, 45 (1997).

60. K. M. Beardmore and N. Grønbech-Jensen, *An Efficient Molecular Dynamics Scheme for the Calculation of Dopant Profiles due to Ion Implantation*, Phys. Rev. E **57**, 7278 (1998).

61. K. Nordlund, *Molecular dynamics simulation of ion ranges in the 1 – 100 keV energy range*, Comput. Mater. Sci. **3**, 448 (1995).

62. K. Nordlund, *Molecular Dynamics Simulation of Atomic Collisions for Ion Irradiation Experiments*, Acta Polytechnica Scandinavica, Applied Physics Series **202**, 1 (1995), PhD thesis, University of Helsinki.

63. D. Cai, N. Grønbech-Jensen, C. M. Snell, and K. M. Beardmore, *Phenomenological electronic stopping-power model for molecular dynamics and Monte Carlo simulation of ion implantation into silicon*, Phys. Rev. B **54**, 17147 (1996).

64. M. J. Puska and R. M. Nieminen, *Atoms embedded in an electron gas: Phase shifts and cross sections*, Phys. Rev. B **27**, 6121 (1983).

65. M. Deutsch, *Electronic charge distribution in crystalline silicon*, Phys. Rev. B **45**, 646 (1992).

66. Z. W. Lu, A. Zunger, and M. Deutsch, *Electronic charge distribution in crystalline diamond, silicon and germanium*, Phys. Rev. B **47**, 9385 (1993).

67. E. Clementi and C. Roetti, *Roothaan-Hartree-Fock atomic wavefunctions*, Atomic Data and Nuclear Data Tables **14**, 177 (1974).

68. R. Wilson, *Random and channeled implantation profiles and range parameters for P and Al in crystalline and amorphized Si*, J. Appl. Phys **60**, 2797 (1986).

69. R. Wilson, D. M. Jamba, P. K. Chu, C. G. Hopkins, and C. J. Hitzman, *Atom and acceptor depth distributions for alumum channeled in silicon as a function of ion energy and crystal orientation*, J. Appl. Phys **60**, 2806 (1986).

70. V. A. Elteckov, D. S. Karpuzov, Y. V. Martynenko, and V. E. Yurasova, in *Atomic Collision Phenomena in Solids*, edited by D. Palmer, M. W. Thompson, and P. D. Townsend (North-Holland, Amsterdam, 1970), Chap. ion penetration into Si single crystal, p. 657.

71. D. Cai, C. M. Snell, K. M. Beardmore, and N. Grønbech-Jensen, *Simulation of phosphorus implantation into silicon with a single parameter electronic stopping power model*, International J. Modern Physics C **9**, 459 (1998).

72. A. Salin, A. Arnau, P. M. Echenique, and E. Zaremba, *Dynamic nonlinear screening of slow ions in an electron gas*, Phys. Rev. B **59**, 2537 (1999).

73. K. M. Klein, C. Park, and A. F. Tasch, *Modeling of cumulative damage effects on ion-implantation profiles*, Nucl. Instr. Meth. Phys. Res. B **59**, 60 (1991).

74. G. Hobler, A. Simionescu, L. Palmetshofer, C. Tian, and G. Stringeder, *Boron channeling implantations in silicon: modeling of electronic stopping and damage accumulation*, J. Appl. Phys. **77**, 3697 (1995).

75. M. Posselt, *Improving the understanding of ion-beam-induced defect formation and evolution by atomistic computer simulations*, Mat. Res. Soc. Symp. Proc. **647**, (2001).

76. Y. Chen, B. Obradovic, M. Morris, and G. Wang *et al.*, *Monte Carlo simulation of heavy species (Indium and Germanium) ion implantation into Silicon*, Journal of technology computer aided design (1999).

77. R. Aderjan and H. Urbassek, *Molecular-dynamics study of craters formed by energetic Cu cluster impact on Cu*, Nucl. Instr. Meth. Phys. Res. B **164**, 697 (2000).

78. V. N. Popok, S. V. Prasalovich, and E. E. B. Campbell, *Nanohillock formation by impact of small low-energy clusters with surfaces*, Nucl. Instr. Meth. Phys. Res. B **207**, 145 (2003).

79. I. Yamada, J. Matsuo, Z. Insepov, T. Aoki, T. Seki, and N. Toyoda, *Nano-processing with gas cluster ion beams*, Nucl. Instr. Meth. Phys. Res. B **164**, 944 (2000).

80. I. Yamada, H. Usui, and T. Takagi, *Bombarding effects by ionized cluster beams*, Nucl. Instr. Meth. Phys. Res. B **33**, 108 (1988).

81. V. I. Shulga and P. Sigmund, *Penetration of slow gold clusters through silicon*, Nucl. Instr. Meth. Phys. Res. B **47**, 236 (1990).

82. P. Sigmund, *Interplay between computer simulation and transport theory*, J. Vac. Sci. Technol. A **7**, 588 (1989).

83. V. I. Shulga, M. Vicanek, and P. Sigmund, *Pronounced nonlinear behavior of atomistic collision sequences induced by keV-energy heavy ions in solids and molecules*, Phys. Rev. A **39**, 3360 (1989).

84. N. Arista, *Stopping of molecules and clusters*, Nucl. Instr. Meth. Phys. Res. B **164**, 108 (2000).

85. K. Nordlund and R. S. Averback, *Atomic displacement processes in irradiated amorphous and crystalline silicon*, Appl. Phys. Lett. **70**, 3103 (1997).

86. K. Nordlund, M. Ghaly, R. S. Averback, M. Caturla, T. Diaz de la Rubia, and J. Tarus, *Defect production in collision cascades in elemental semiconductors and FCC metals*, Phys. Rev. B **57**, 7556 (1998).